2. V. L. Dragun, and S. A. Filatov, Temperature Measurements using Thermovision Equipment [in Russian], Preprint No. 23, Institute of Heat and Mass Transfer, Academy of Sciences of the Belorussian SSR, Minsk (1986).
3. V. L. Dragun, V. A. Zavadskii, and S. A. Filatov, "Heat and mass transfer in porous bodies," pp. 167-172 in: Collection of Scientific Papers of the Institute of Heat and Mass Transfer, Academy of Sciences of the Belorussian SSR, Minsk (1983).
4. V. L. Dragun, S. V. Konev, and S. A. Filatov, Thermographic Investigations of Heat Pipes and Heat Exchangers Based on Them [in Russian], Preprint No. 33, Institute of Heat and Mass Transfer, Academy of Sciences of the Belorussian SSR, Minsk (1987).

HYDRODYNAMICS, HEAT AND MASS TRANSFER, AND SOLIDIFICATION IN THE FORMATION OF INGOTS AND CASTINGS

F. V. Nedopekin

UDC 536.42

A set of interrelated mathematical models is developed for processes of heat and mass transfer and solidification. Its scope is illustrated on specific examples of the calculation of cast-ingot formation.

The quality of metal is determined, to a considerable extent, by the interrelated processes of hydrodynamics, heat and mass transfer, and solidification in the period of transition from the liquid to the solid state.

The most acceptable investigation procedure in this case is mathematical modeling, as an effective instrument in the study, prediction, and optimization of complex nonlinear transfer processes occurring in solidifying alloys.

A generalized mathematical model of conjugate processes of momentum, heat, and mass transfer in the solidification of an Fe–C binary melt, taking account of the two-phase zone (TPZ), is formulated from the perspective of continuum thermomechanics [1], and includes averaged macrocontinuum equations of motion, heat transfer, mass transfer, continuity, magnetic induction (noninductive approximation), and electric-charge balance and the equilibrium condition at the boundary between melt and solid phase (the equation for the liquidus line in accordance with the quasi-equilibrium theory of the two-phase zone [2])

$$\rho_2\left[\frac{\partial\langle \mathbf{U}_2\rangle}{\partial t}+\left(\frac{\langle \mathbf{U}_2\rangle}{1-\xi}\nabla\right)\langle \mathbf{U}_2\rangle\right]=-\nabla\langle P_2\rangle+$$
$$+\mu\Delta\langle \mathbf{U}_2\rangle+\mathbf{g}\langle\rho_2\rangle-\frac{\mu}{k(\xi)}\langle \mathbf{U}_2\rangle+\langle(\mathbf{j}\times\mathbf{B})_2\rangle; \quad (1)$$

$$[(c_1\rho_1-c_2\rho_2)\xi+c_2\rho_2]\frac{\partial T}{\partial t}+\nabla(c_2\rho_2T\langle \mathbf{U}_2\rangle)=\nabla[\lambda_1-\lambda_2)\xi+\lambda_2]\nabla T+$$
$$+L\rho_1\frac{\partial\xi}{\partial t}\pm Q; \quad (2)$$

$$(1-\xi)\frac{\partial C_2}{\partial t}+\nabla(C_2\langle \mathbf{U}_2\rangle)=\nabla[D_2(1-\xi)\nabla C_2]+k_*C_2\frac{\partial\xi}{\partial t}; \quad (3)$$

$$\frac{\partial}{\partial t}[\xi\rho_1+(1-\xi)\rho_2]+\nabla[(1-\xi)\rho_2\langle \mathbf{U}\rangle_2]=0; \quad (4)$$

Donetskii State University. Translated from Inzhenerno-Fizicheskii Zhurnal, Vol. 57, No. 3, pp. 450-458, September, 1989. Original article submitted July 1, 1988.

0022-0841/89/5703-1073$12.50

$$\frac{\partial \langle \mathbf{B}_2 \rangle}{\partial t} = \nu_m \Delta \langle \mathbf{B}_2 \rangle; \tag{5}$$

$$\operatorname{div} \langle \mathbf{j}_2 \rangle = 0; \tag{6}$$

$$T = -\alpha C_2 + T_C. \tag{7}$$

On the basis of the generalized mathematical model in Eqs. (1)-(7), particular models of hydrodynamic and thermophysical processes in the filling of a mold by a syphon and from above and more complex molds with various methods of melt supply and solidification, for cast objects of three groups: ingots broadened at the top and bottom and large castings (of mass $m \sim 2 \cdot 10^3$-$8 \cdot 10^3$); 2) small ($m \sim 0.2$ kg) irregularly shaped objects in casting with a smeltable model (CSM); 3) cylindrical ingots from the electroslag melting (ESM) of metallized droplets ($m \sim 30$-40 kg).

The mathematical model of the pouring stage is written in the Boussinesq approximation, under the assumption that the surface is level, plane, and heat insulated, the contact between the mold wall and the melt is ideal, and there is no redistribution of impurity in view of the short duration of pouring [3]. Turbulence is taken into account by introducing an effective kinematic viscosity ν_e and thermal diffusivity a_e, reflecting the molecular and turbulent momentum and heat transfer. Therefore, the model takes the form of a system of equations of motion in Navier–Stokes form, heat transfer, heat conduction for the mold casting mold) walls, and continuity; in dimensionless variables, when $\xi = 0$, the system is as follows

$$\frac{\partial \mathbf{V}}{\partial \mathrm{Fo}} + \mathrm{Pe}\,(\mathbf{V}\nabla)\,\mathbf{V} = -\mathrm{Eu}\,\mathrm{Pe}\,\nabla\pi + \mathrm{Pr}_e \Delta \mathbf{V} + \mathbf{e}_y \frac{\mathrm{Gr}_T \mathrm{Pr}_e}{\mathrm{Pe}}\,\Theta; \tag{8}$$

$$\frac{\partial \Theta}{\partial \mathrm{Fo}} + \mathrm{Pe}\,(\mathbf{V}\nabla)\,\Theta = \frac{a_e}{a_2}\,\Delta\Theta; \tag{9}$$

$$\frac{c_i \rho_i}{c_2 \rho_2}\,\frac{\partial \Theta}{\partial \mathrm{Fo}} = \nabla\left(\frac{\lambda_i}{\lambda_2}\,\nabla\Theta\right); \tag{10}$$

$$\nabla \mathbf{V} = 0. \tag{11}$$

Generalized representation of the boundary conditions permits the modeling of: a) the filling of a mold by a syphon and from above; three-jet filling from below, four-jet filling from above, lateral filling, simultaneous filling from above and below, and other forms of mold filling. The kinetics of the solid skin is predicted here on the basis of the isotherm corresponding to the solidification temperature of the melt: $\Theta_* = 0{,}5(\Theta_л + \Theta_c)/2$.

The above classification of cast parts is the result of various factors determining the hydrodynamic configuration in solidificationafter the pouring stage. In the first group, thermoconcentrational convection is determining ($\mathrm{Gr_T Pr} >> 10^3$); filtrational flow on account of phase shrinkage is negligibly small, and there is no electrovortex flow (EVF) due to the interaction of the melt current with the intrinsic magnetic field in the ESM, i.e., the fourth and fifth terms on the right-hand side of Eq. (1) vanish. The model includes Eqs. (1)-(4), (7), and (10), and is written in dimensionless form in the variables ($\langle\omega\rangle$, $\langle\psi\rangle$) [4, 5]:

$$\frac{\partial \langle \omega \rangle}{\partial \mathrm{Fo}} + [(1-\xi)\langle \mathbf{V} \rangle_2 \nabla]\langle \omega \rangle = \mathrm{Pr}\,\nabla(\nu_* \nabla \langle \omega \rangle) - (1-\xi)\,\mathrm{Pr}^2 \left(\mathrm{Gr}_T \frac{\partial \Theta}{\partial x} + \mathrm{Gr}_D \frac{\partial S}{\partial x}\right); \tag{12}$$

$$c_* \frac{\partial \Theta}{\partial \mathrm{Fo}} + (1-\xi)(\langle \mathbf{V} \rangle_2 \nabla)\,\Theta = \nabla[(1+\lambda\xi)\nabla\Theta]; \tag{13}$$

$$(1-\xi)\left[\frac{\partial S}{\partial \mathrm{Fo}} + (\langle \mathbf{V} \rangle_2 \nabla)\,S\right] = \mathrm{Lu}\,\nabla[(1-\xi)\nabla S] + (1-k_0)\,S\,\frac{\partial \xi}{\partial \mathrm{Fo}}; \tag{14}$$

$$\Delta \langle \psi \rangle = -\langle \omega \rangle; \tag{15}$$

$$\Theta = -\varphi_0 S + \Theta_C. \tag{16}$$

In the second group of cast components, the role of thermoconcentrational convection in the liquid "core" (in view of the small mass of the casting) becomes practically zero ($Gr_T Pr \cdot \leq 10^3$-10^4). However, the role of thermofiltrational flow within the TPZ increases, and may be determining in the formation of porosity in the casting. Taking account of the small Reynolds numbers inside the TPZ and the absence of EVF, Eq. (1) reduces to a modified Darcy's flow law, which is transformed by means of Eq. (4) to Poisson's equation for the pressure; note that the model is formulated in the physical variables ($\langle V \rangle_2$, π)) [6]:

$$\nabla\left(\frac{\mathrm{Da}}{\mathrm{Pr}}\nabla\pi\right) = \rho_* \frac{\partial\xi}{\partial \mathrm{Fo}} - \\ - \mathrm{Pr}\frac{\partial}{\partial y}\left\{\mathrm{Da}(1-\xi)\left[(1-\Theta)\,\mathrm{Gr}_T - \mathrm{Ga}\,y\frac{\partial\xi}{\partial y}\right]\right\}. \tag{17}$$

Together with Eqs. (13), (14), and (16), Eq. (17) is the basis of the mathematical model of the CSM solidification of ingots.

The uniqueness conditions include: the geometric parameters of the region reflecting the size and shape of the given ingots and castings; the thermophysical parameters corresponding to solidification of ingots of bubble-free steel St3sp in a cast-iron mold and irregularly shaped castings of steel 35KhL; initial conditions taking account of the hydrodynamic configuration in the ingot–mold system in the casting period; boundary conditions reflecting adhesion and impermeability for the velocity vector, symmetry of the region, heat-insulation of the exothermal charge of the metal "mirror," the formation of a gas gap between the ingot and the mold wall, and the absence of impurity flow in the mold wall.

Cast parts of the third group are formed with the following distinguishing features: a) the hydrodynamic configuration is determined by EVF and thermal convection in slag baths (SB) and metallic baths (MB) (in comparison with the Intensity of these flows, the role of filtration is negligibly small; b) the thermal configuration is complicated by the presence of Joule heat and heat sinks in the pellet and the alloy (Q). Therefore, the mathematical model consists of the complete system in Eqs. (1)-(7) written in the variables (ω, ψ) in the cylindrical coordinate system, taking into account that the fourth term on the right-hand side of Eq. (1), which takes the following form for SB

$$\frac{\partial\omega}{\partial \mathrm{Fo}} + v_r\frac{\partial\omega}{\partial r} + v_z\frac{\partial\omega}{\partial z} - \frac{v_r}{r}\omega = \mathrm{Pr}\,\Delta\omega + \left(\mathrm{Gr}_T\frac{\partial\Theta}{\partial r} - 2\tilde{S}\,\frac{b}{r}\,\frac{\partial b}{\partial z}\right)\mathrm{Pr}^2; \tag{18}$$

$$\frac{(c\rho)_{sl}}{c_2\rho_2}\left(\frac{\partial\Theta}{\partial \mathrm{Fo}} + v_r\frac{\partial\Theta}{\partial r} + v_z\frac{\partial\Theta}{\partial z}\right) = \nabla\left(\frac{\lambda_{sl}}{\lambda_2}\nabla\Theta\right) + \frac{r_0^2}{T_2^0\lambda_2}(q_J - q); \tag{19}$$

$$\frac{\partial}{\partial r}\left(\frac{1}{r}\,\frac{\partial\psi}{\partial r}\right) + \frac{\partial}{\partial z}\left(\frac{1}{r}\,\frac{\partial\psi}{\partial z}\right) = \omega; \tag{20}$$

$$\Delta\varphi = 0; \tag{21}$$

$$\mathrm{Pr}_*\frac{\partial b}{\partial \mathrm{Fo}} = \Delta b, \tag{22}$$

is zero; here the subscript sl denotes the slag.

The hydrodynamics in MB is described by Eq. (12) with the introduction of EVF; the heat transfer in the solidifying ingot and the electrode is described by Eqs. (13)-(14), (16), and (10).

The uniqueness conditions given above now require the addition of boundary conditions for the magnetic induction and the electric potential. The model in Eqs. (18)-(22) describes the momentum, heat, mass, and charge transfer in the casting–electrode–slag–pellet–crystallization-unit system.

The use of Eq. (16) also permits conversion from the mass-transfer Eq. (14) to the equation for the proportion of solid phase ξ, which is common to all the particular models

$$k_* (\Theta_C - \Theta) \frac{\partial \xi}{\partial \mathrm{Fo}} + [\mathrm{Lu} \nabla\Theta + (\Theta - \Theta_K) \langle \mathbf{V} \rangle_2] \nabla\xi = \\ = \left\{ \mathrm{Lu} \Delta\Theta - \nabla [(\Theta_C - \Theta) \langle \mathbf{V} \rangle_2] - \frac{\partial \Theta}{\partial \mathrm{Fo}} \right\} (1 - \xi). \tag{23}$$

The construction of a computational algorithm for the given mathematical models, taking account of the conjugacy and nonlinearity of the boundary problem, is based on the use of the following sequence of finite-difference methods: the method of variable directions or the locally homogeneous scheme; the method of "perturbed coefficients"; and the integrointerpolational method. The use of these methods is illustrated for the example of a model differential equation of general form [4]. The final stage in the development of finite-difference analogs is to construct a Samarskii implicit monotonic difference scheme, ensuring second-order approximation with respect to the coordinate and first-order with respect to the time [7]. The algorithm for calculating the solidification problem taking account of the TPZ consists of two parts: the thermal and hydrodynamic problems. In the thermal problem, an iterative scheme of taking nonlinearity into account is used [8].

In calculating the filtrational flow of melt in the TPZ of a solidifying casting of irregular shape, utilization of the method of hypothetical regions is proposed [9]. This permits the elimination of a series of computational and programmatic difficulties in organizing the fitting of Poisson's equation relative to the pressure in the multiphase filtration region.

Finite-difference analogs are constructed in nonuniform space–time grids. With the aim of increasing the accuracy of the approximation for regions of complex configuration, the method of step modeling of the boundary is used. This allows the difference in slopes of the internal and external surfaces of the mold, the geometric parameters of the heat-insulation bushes, the conical form of the deadhead attachment, and the complex configuration of the irregularly shaped casting to be taken into account with the required accuracy [10].

For the example of casting a 5-ton steel ingot, thermomechanical convection due to temperature inhomogeneity of the melt and the mechanical action of the casting jet is investigated. It is shown that, in the solidifying phase of the casting, the difference in the intensity of melt motion in thermomechanical and purely induced convection is ~3%, and the corresponding figure for the thermal energy is ~0.05%, apart from the dependence on T_3^0 and the rate of pouring ε'. It may be concluded that the contribution of thermal convection to heat transfer between the melt and the mold in the filling period is negligibly small.

The hydrodynamics and heat transfer in the filling of a mold by a syphon and from above is now investigated (Fig. 1a-c). In the specific range of technological parameters of casting, it is found that the inhomogeneous vortex structure of the flow plays the principal role in heat transfer between the melt and the mold. It is due to the nonmonotonic heat flux (Nusselt number Nu) along the mold surface, and consequently the formation of a solid "skin" of nonuniform thickness.

In studying the features of filling as a function of the pouring rate and T_3^0, it is found that four-fold increase in the pouring rate is accompanied by decrease in thickness of the solid skin and its uniformity, the region of greatest variation in thermal stress at the mold wall, and the heat losses, and by increase in Nu (by ~7%) at the mold wall (Fig. 1c) and the thermal stress there. Increase in T_3^0 to 523 K faciliates a decrease in Nu (by 6%), heat losses, thermal stress, and "thermal" shock at the internal surface of the mold [3].

It is found that the rational filling conditions in the given range of technological parameters of casting are as follows: $\varepsilon' = 0.0052$ m/sec, $T_3^0 = 523$ K, and initial melt temperature $T_2^0 = 1833$ K with syphon filling; rate of melt outflow from the reservoir 7 m/sec, $T_3^0 = 493$ K, $T_2^0 = 1833$ K, and ingot height $L_2 = 0.6$-2.4 m for filling from above.

Investigation of the hydrodynamic and thermophysical processes with various methods of filling the molds for casting hydroturbine blades (Fig. 1d,e) and the frame of a steam turbine (Fig. 1f,g) leads to satisfactory agreement of the results of computational experiment (CE) and physical modeling [11]. For three-jet filling, it is found that: the small-vortex structure of the flow transforms to a large-vortex structure as filling proceeds; at the moment

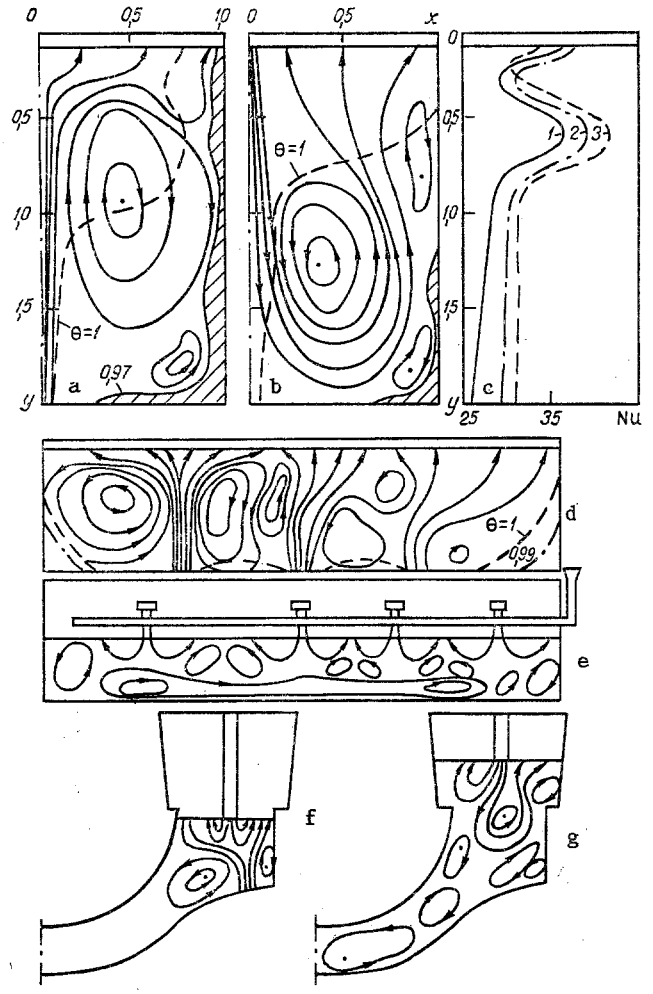

Fig. 1. Streamlines and isotherms in the filling of a mold by a syphon (a) and from above (b) and in the filling of more complex molds (d-g); distribution of heat flux at the internal surface of the mold (c): 1) $\varepsilon' = 0.005$ m/sec, $T_3^0 = 532$ K; 2) 0.005, 293; 3) 0.0208, 293.

that pouring ceases, the multivortex structure is degenerate; the loss of thermal energy is ~0.1%; no solid skin is formed on the surface of the mold.

CE confirms that the rational conditions in three-jet filling, from the viewpoint of reducing the sections of greatest erosion of the casting mold, are conditions with equal flow rates in the three jets; the most favorable hydrodynamic configuration in the blade mold is achieved with lateral filling.

For a rectangular ingot of low-carbon steel with Gr_D and Gr_T in the range $2 \cdot 10^7$-$7 \cdot 10^9$, relative height ℓ_2 = 2-6, and ε' = 0.0052-0.0208 m/sec when x_0 = 0.3 m, the features of thermoconcentrational and mixed convection due to the residual action of the casting jet and the thermoconcentrational inhomogeneity are investigated (Fig. 2). It is established that mixed convection also develops in three stages: the first consists of slowing of the motion induced by the casting jet and the predominance of thermal convection; the second and third stages are also characterized by vibrational flow of the melt. However, the amplitude of the vibrations is larger here than for thermoconcentrational convection. The influence of thermoconcentrational and mixed convection on the formation of chemical inhomogeneity of the ingot is shown. Convection is responsible for the impurity enrichment of the axial and upper parts of the casting. The most critical stage in natural convection in the formation of chemical inhomogeneity of the ingot is the transitional stage. In this stage, impurity accumulates in the liquid phase at the interface between the "concentrational" and "thermal" vortices, and consequently bands with an increased carbon content in the solid phase are formed (Fig. 2d-f). Satisfactory agreement, of the CE results with physical-modeling data is observed for the naphthalene–methanol system.

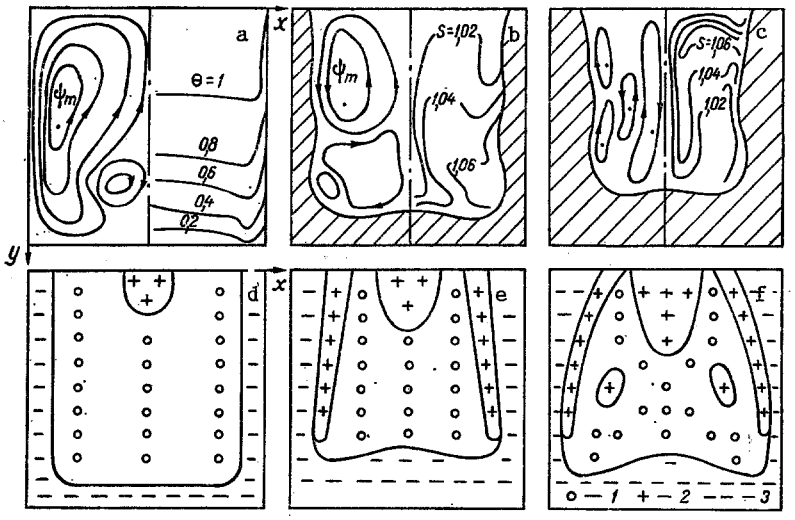

Fig. 2. Current (on the left), temperature, and concentration isolines in a melt for three stages of thermoconcentrational convection (a-c) and zones of degree of liquation $S_* = (C_1 - C_0)/C_0$ in the ingot (d-f): d) no convection; e) with mixed convection; f) physical modeling: 1) $S_* = 0$; 2) $S_* > 0$; 3) $S_* < 0$.

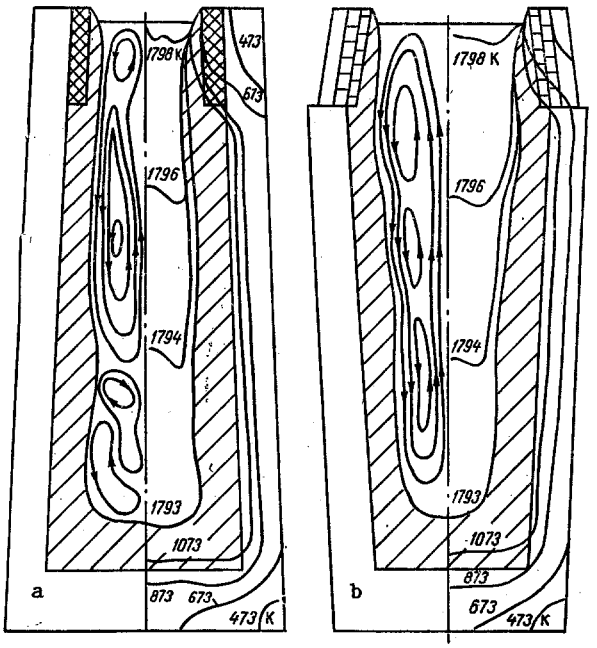

Fig. 3. Streamlines (on the left) and isotherms in a steel casting broadened at the bottom (a) and at the top (b); t = 20 min.

In investigating the influence of the casting jet on the impurity distribution in the ingot some increase in the negative liquation in the peripheral region of the ingot and positive liquation in the band of increased carbon contact is noted, as well as shift of this band toward the periphery of the region.

The interrelated hydrodynamic and heat- and mass-transfer processes in the formation of 8-ton steel ingots broadened at the top and the bottom are investigated as a function of the intensity of heating of the upper part by the heat-insulation bushes (Fig. 3) [4, 5, 10]. Convection leads to increase in heat content of the deadhead section of the casting. It is found that improvement in the heat insulation and increase in height of the bush leads to

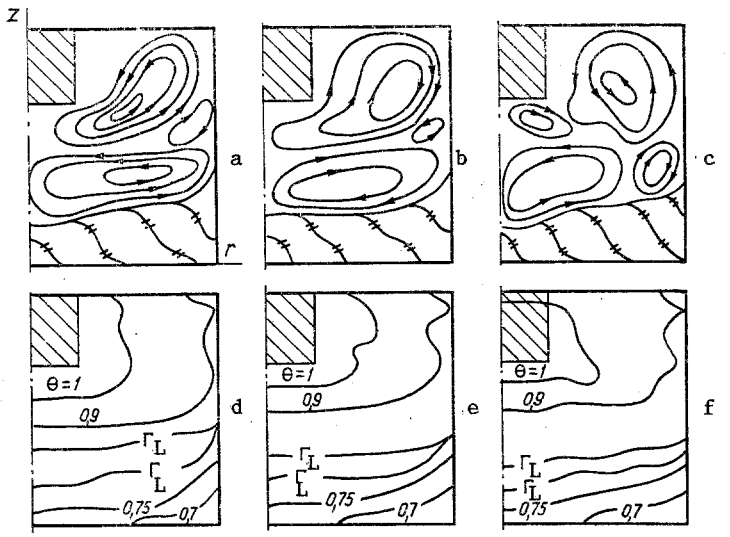

Fig. 4. Streamlines (a-c) and isotherms (d-f) in ESM casting: a) purely electrovortex convection; b, e) purely thermal convection; c, f) thermal and electrovortex convection; g) no convection.

reduction in convection rate, heat content of the mold, and cooling rate of the ingot and to increase in heat content of the deadhead, pronounced reduction in depth of the open shrinkage cavity, and slight reduction in volume of the closed shrinkage cavity. The influence of the convective heat transfer between the deadhead and the ingot body on the formation of shrinkage cavities is more significant than the influence of the increase in the heat-insulation properties of the bushes in the given range.

In investigating the thermophysical processes in the solidification of irregularly shaped castings made from low-alloy steel in ceramic molds and of cylindrical ingots from instrument 1 steels in water-cooled ESM crystallization units [6, 12], it is shown that thermofiltrational flow is directed basically toward the jet boundary; the velocity is no more than 10^{-4}-10^{-5} m/sec. The pressure in the melt does not reach values corresponding to the formation of gas-shrinkage porosity in warm conditions (preliminary heating of the model) of CSM ingot formation. Heat transfer on account of filtration leads to some increase in temperature (to 2.3% of the solidification interval of the binary melt) and reduction in the proportion of solid phase in the TPZ and also to slowing of penetration of the characteristic TPZ boundaries.

It is found that (Fig. 4), in the solidification of cylindrical ESM castings of metallized pellets, the hydrodynamic configuration in the slag and metal baths is determined by the superposition of electrovortex and metallic convection; the flow has a multivortex structure. Thermal convection has a positive role – decreasing the TPZ width – and electrovortex convection has a negative role – increasing the depth of the liquid hole, which is responsible for the development of porosity and liquation in the cast ingot. It is shown that heat transfer through the floor has almost no influence on the temperature distribution in the casting when its height is considerable; the component of the temperature gradient in the axial direction is higher than in the radial direction, which leads to an analogous relation between the axial and radial thermal stress. The greatest density of the distribution of equipotential lines and elevated liberation of Joule heat is observed at the electrode surface and at the slag–metal boundary.

NOTATION

$\Theta = T/T_2^0$, $S = C/C_0$, $\mathbf{V} = \mathbf{U}/u_0$, $\mathrm{Fo} = ta_2/x_0^2$, π, x, y, b, dimensionless temperature, impurity concentration, velocity, time, pressure, horizontal and vertical coordinate, and induction of magnetic field; T, C, $\mathbf{U}$, P, t, $\mathbf{j}$, $\mathbf{B}$, dimensional temperature, concentration, velocity, pressure, time, electric current density, and induction of the magnetic field; T_2^0, T_3^0, C_0, initial temperature of melt and mold and concentration; $u_0 = a_2/x_0$, x_0, characteristic velocity and coordinate; $\mathrm{Gr_T} = g\beta_T T_2^0 x_0^3/\nu^2$, $\mathrm{Gr_D} = g\beta_D C_0 x_0^3/\nu^2$, $\mathrm{Pr} = \nu/a_2$, $\mathrm{Pe} = \mu_0 x_0/a_2$, $\mathrm{Ga} = gx_0^3/\nu^2$, $\mathrm{Eu} = P_0/\rho_2 u_0^2$, $\mathrm{Lu} = D_2/a_2$, thermal and diffusional Grashof numbers, Prandtl, Peclet, Galileo, Euler,

and Lewis numbers; ρ, density; α, slope of liquidus line on state diagram; ν, μ, a, λ, k, D_2, c, k_0, ν_m, β_T, β_D, kinematic viscosity, dynamic viscosity, thermal diffusivity, thermal conductivity, permeability, diffusion coefficient, specific heat, impurity distribution coefficient, magnetic viscosity, and coefficients of thermal and concentrational volume expansion; g, acceleration due to gravity; θ_L, θ_S, θ_C T_C, liquidus, solidus, and crystallization temperatures; $k_* = 1 - k_0\rho_1/\rho_2$; $\langle U_2\rangle$, $\langle P_2\rangle$, $\langle\rho_2\rangle$, $\langle(j \times B)_2\rangle$, volume means of quantities in the liquid phase; $\langle U\rangle_2$ true volume mean velocity of liquid phase; L, latent heat of phase transition; $Da = k/x_0^2$, $Pr_m = \nu_m/\nu$ Darcy's number and magnetic Prandtl number; $Pr* = Pr_m/Pr$; S, electrovortex-flow parameter; v_r, v_z, r, z, φ, dimensionless radial and vertical velocity components and coordinates, electric potential; $Pr_e = Pr\nu_e/\nu$; $\langle V\rangle_2$ $\langle\omega\rangle$, $\langle\psi\rangle$ dimensionless true volume mean velocity, volume mean vortex velocity, and volume mean current function of the liquid phase; $\varphi_0 = \alpha C_0/T_2^0$; $K = L/(c_2T_2^0)$; $c_* = 1 + (c_1/c_2 - 1)\xi - K\partial\xi/\partial\Theta$; $\lambda = \lambda_1/\lambda_2 - 1$; $\rho_* = \rho_1/\rho_2 - 1$; q_J, q, dimensionless power of Joule heating and heat sinks in the pellet and the alloy; r_0, radius of ESM ingot; $\nu* = \nu*(\xi)$, effective kinematic viscosity [4]. Indices: 1, solid phase; 2, melt; 3) ingot mold (mold); 4) heat-insulation bushes.

LITERATURE CITED

1. R. I. Nigmatulin, Principles of Mechanics of Heterogeneous Media [in Russian], Moscow (1978).
2. V. T. Borisov, Theory of Two-Phase Zone of Metallic Casting [in Russian], Moscow (1987).
3. I. L. Povkh, F. V. Nedopekin, and V. V. Belousov, Dokl. Akad. Nauk UkrSSR, Ser. A, No. 9, 82-85 (1986).
4. F. V. Nedopekin and S. S. Petrenko, Insh. Fiz. Zh., 97, No. 2, 286-293 (1984).
5. F. V. Nedopekin and S. S. Petrenko, Teplofiz. Vys. Temp., 23, No. 3, 549-555 (1985).
6. F. V. Nedopekin and V. S. Borodin, Izv. Akad. Nauk SSSR, Met., No. 5, 216-222 (1987).
7. A. A. Samarskii, Theory of Difference Schemes [in Russian], Moscow (1977).
8. L. A. Kozdoba, Solution of Nonlinear Heat-Conduction Problems [in Russian], Kiev (1976).
9. I. L. Povkh, F. V. Nedopekin, and V. S. Borodin, Dokl. Akad. Nauk UkrSSR, Ser. A, No. 8, 38-40 (1985).
10. F. V. Nedopekin, S. S. Petrenko, V. F. Polyakov, and V. Ya, Minevich, Izv. Akad, Nauk SSSR, Met., No. 5, 64-69 (1985).
11. E. D. Taranov et al., Investigation of Hydrodynamic Processes in the Casting of Irregularly shaped Ingots [in Russian], Kiev (1984).
12. V. S. Borodin, V. M. Melikhov, F. V. Nedopekin, et al., Izv. Vyssh. Uchebn. Zaved., Chern. Met., No. 7, 72-76 (1987).

STRUCTURAL PARAMETRIC METHOD OF IDENTIFICATION OF MATHEMATICAL MODELS OF TECHNOLOGICAL PROCESSES

P. V. Sevast'yanov

UDC 536.24

A method is proposed for simultaneous estimation of the model parameters and their quality according to a set of criteria. Models of solidification in a chill mold are considered as an example.

The distinguishing singularity of any sufficiently complex technological process is the possibility of development of a whole series of competing models for its mathematical description, that could formally be represented in the form $Y = f(X, \Theta)$. In addition to the parameteric identification problems here, the estimate of Θ using models and test data, questions of structural identification, i.e., selection of the best model out of the available set, also occur.

As is mentioned in [1], these problems are interrelated since there is no sense in comparing models for accuracy prior to estimation of the parameters, and refining the parameters of a model of inadequate structure.

Translated from Inzhenerno-Fizicheskii Zhurnal, Vol. 57, No. 3, pp. 459-463, September, 1989. Original article submitted March 23, 1988.

0022-0841/89/5703-1080$12.50